

FIRST LASING OF THE IR FEL AT THE FRITZ-HABER-INSTITUT, BERLIN

W. Schöllkopf, S. Gewinner, W. Erlebach, G. Heyne, H. Junkes, A. Liedke, V. Platschkowski, G. von Helden, W. Zhang, G. Meijer, Fritz-Haber-Institut der Max-Planck-Gesellschaft, Berlin, Germany
 H. Bluem, M. Davidsaver*, D. Dowell*, K. Jordan*, R. Lange*, H. Loos*, J. Park, J. Rathke,
 A.M.M. Todd, L.M. Young*, Advanced Energy Systems, Medford, NY, USA
 U. Lehnert, P. Michel, W. Seidel, R. Wünsch, HZDR, Rossendorf, Germany
 S.C. Gottschalk, STI Optronics, Bellevue, WA, USA

Abstract

A new mid-infrared FEL has been commissioned at the Fritz-Haber-Institut in Berlin. The oscillator FEL operates with 15 – 50 MeV electrons from a normal-conducting S-band linac. Calculations of the FEL gain and IR-cavity losses predict that lasing will be possible in the wavelength range from less than 4 to more than 50 μm . First lasing was achieved at a wavelength of 16 μm with an electron energy of 28 MeV. At these conditions, lasing was observed over a cavity length scan range of 100 μm .

INTRODUCTION

At the Fritz-Haber-Institut in Berlin, Germany, a new IR and THz FEL has been commissioned for applications in gas-phase spectroscopy of (bio-)molecules, clusters, and nano-particles, as well as in surface science [1-3]. To cover the wavelength range of interest from about 4 to

500 μm , the system design, shown in Fig. 1, includes two FELs; a mid-infrared (MIR) FEL for wavelengths up to about 50 μm and a far-infrared (FIR) FEL for wavelengths larger than about 40 μm . A normal conducting S-band linac provides electrons of up to 50 MeV energy to either FEL.

As of August 2012, installation of the accelerator and electron-beam transport system (designed and installed by Advanced Energy Systems, Inc.) [4,5], the MIR undulator (STI Optronics) [6], and the MIR oscillator mirror optical equipment (Bestec GmbH) is complete and commissioning is ongoing, whereas the FIR FEL has not yet been installed. In this paper, after a brief summary of the electron accelerator, we describe the design of the MIR FEL and report on results from first lasing achieved on February 14th, 2012.

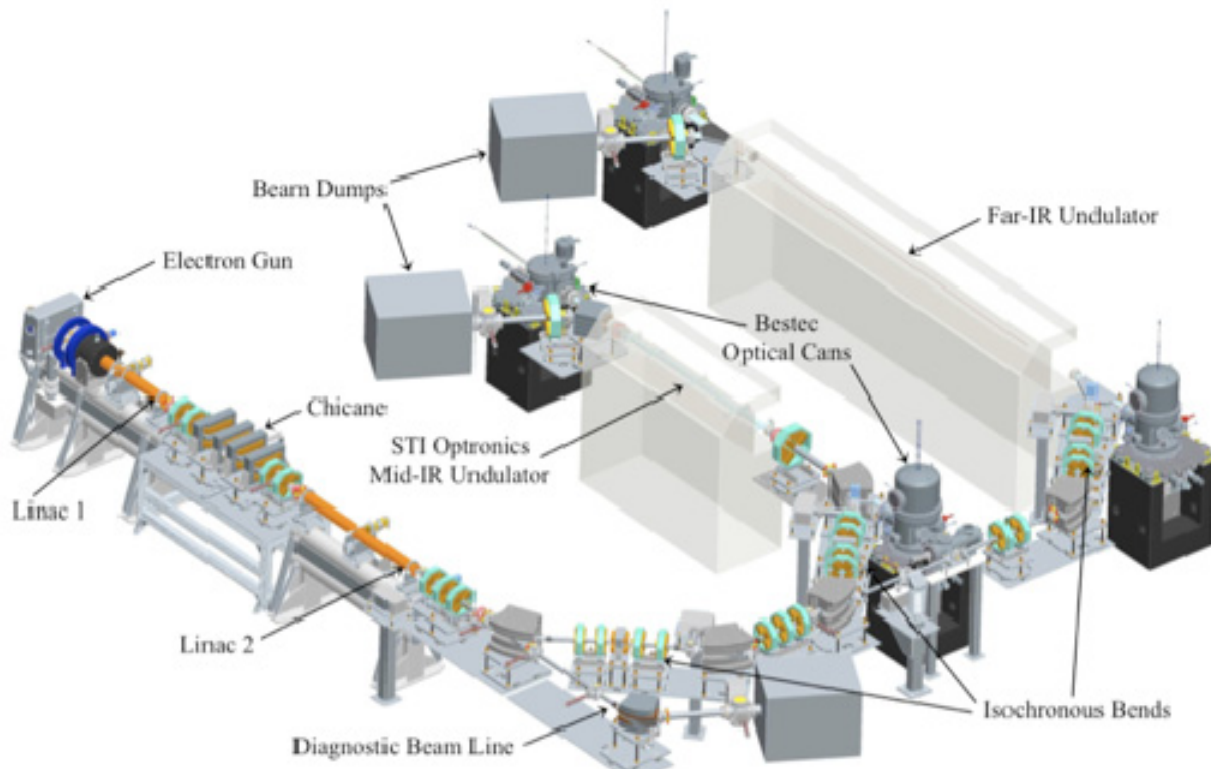


Figure 1: Schematic overview of the infrared free-electron laser at the Fritz-Haber-Institut.

* Consultants to AES

ELECTRON ACCELERATOR

In Table 1 we summarize the projected top-level electron beam performance. The design of the accelerator and beam transport system has been described elsewhere [2-5]. In brief, it consists of a 50 MeV accelerator driven by a gridded thermionic gun with a beam transport system that feeds two undulators and a diagnostic beamline. The first of two 3 GHz S-band, normal-conducting electron linacs accelerates the electron bunches to a nominal energy of 20 MeV, while the second one accelerates or decelerates the electrons to deliver any final energy between 15 and 50 MeV. A chicane between the structures allows for adjustment of the bunch length as required.

Table 1: Summary of Electron Beam Parameters

| Parameter | Unit | Specification | Target |
|-------------------------------------|-----------------------|---------------|---------|
| Electron energy | MeV | 20 - 50 | 15 - 50 |
| Energy spread | keV | 50 | < 50 |
| Energy drift per hour | % | 0.1 | < 0.1 |
| Bunch charge | pC | 200 | > 200 |
| Micro-bunch length | ps | 1 - 5 | 1 - 10 |
| Micro-bunch rep. rate | GHz | 1 | 1 |
| Micro-bunch jitter | ps | 0.5 | 0.1 |
| Macro-bunch length | μs | 1 - 8 | 1 - 15 |
| Macro-bunch rep. rate | Hz | 10 | 20 |
| Normalized rms transverse emittance | $\pi \text{ mm mrad}$ | 20 | 20 |

The final design has optimized the specifications of the linac that are most relevant for the IR and THz FEL performance. For instance, the maximum bunch charge of the micro-pulses, which are repeated at rate of up to 1 GHz, has been increased to 300 pC. In addition, the length of the macro-bunches has been increased to 15 μs.

MID-INFRARED OSCILLATOR FEL

Each of the two FELs consists of an undulator placed within an IR cavity as summarized in Table 2. The MIR FEL includes a 2-m-long planar wedged-pole hybrid undulator manufactured by STI Optronics with a period length of 40 mm. A detailed description of the MIR undulator is provided in Ref. [6]. At a minimum gap of nominally 16.5 mm, a maximum root-mean-square undulator parameter K_{rms} of more than 1.6 is reached. This, in combination with the minimum electron energy of 15 MeV corresponds to a maximum wavelength of more than 60 μm (see Fig. 5).

Table 2: Mid-IR and Far-IR FEL Optical Parameters

| Undulator | MIR | FIR |
|------------------|---------------|----------------------|
| Type | Planar hybrid | Planar hybrid or PPM |
| Material | NdFeB | NdFeB or SmCo |
| Period (mm) | 40 | 110 |
| No. of periods | 50 | 40 |
| Length (m) | 2.0 | 4.4 |
| K_{rms} | 0.5 – 1.6 | 1.0 – 3.0 |
| IR-cavity | MIR | FIR |
| Length (m) | 5.4 | 7.2 |
| Waveguide | none | 1-D 10 mm high |

The undulator is placed asymmetrically within a 5.4 m long IR cavity with the undulator position being offset by

50 cm from the cavity center in the direction away from the out-coupling mirror, as depicted schematically in Fig. 2. The reason for the offset is the effect of hole-outcoupling on the optical mode in the cavity. Simulations reveal that, close to the outcoupling hole, a hollow mode can be formed, resulting in a significant reduction of the outcoupled photon flux as compared to a Gaussian mode. Shifting the undulator and, hence, the cavity mode waist 50 cm away from the outcoupling mirror reduces this effect to a negligible level.

Another consequence of hole-outcoupling is that different hole diameters are needed to optimize performance at different wavelengths. Therefore a motorized in-vacuum mirror changer has been installed (see Fig. 3). It permits the precise positioning of either one out of five cavity mirrors with outcoupling-hole

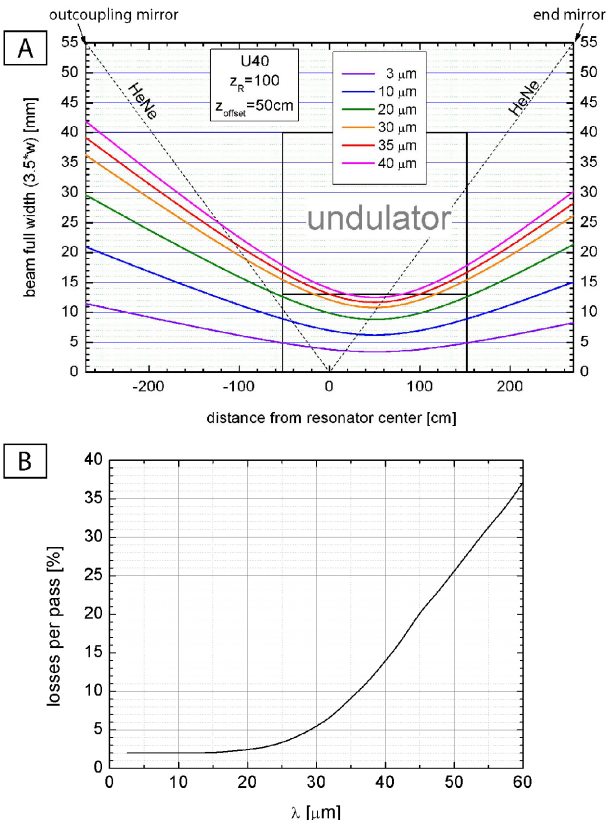


Figure 2: Optical modes and cavity losses in the MIR FEL. In (A) the calculated optical mode widths (defined as the 3.5ω width of the Gaussians) within the cavity are plotted for wavelengths from 3 to 40 μm. The black box labelled ‘undulator’, which is offset by 50 cm from the cavity center, indicates the vertical and horizontal inner clearance of the undulator chamber of 13 and 40 mm, respectively. The dotted line indicates the path of the HeNe beam which is horizontally tilted to the axis. In (B) the cavity losses are plotted as a function of wavelength. The losses are mainly caused by the vacuum chamber in the undulator and self-consistently calculated using the commercial code GLAD. 1% reflectivity loss per mirror is included. Losses due to hole outcoupling are not taken into account.

diameters of 0.75, 1.0, 1.5, 2.5, and 3.5 mm. The mirror at the other cavity end has no hole and is mounted on a precision translation stage to enable cavity length adjustment and, if needed, compensation of thermal drifts. The signal from a HeNe-laser interferometer delivers a feedback signal for cavity length stabilization.

The cavity-end mirror and the outcoupling mirrors are gold-plated copper mirrors of spherical concave shape with a radius of curvature of 2.65 m and 3.51 m, respectively. As a result, the waist of the cavity mode is shifted by 50 cm away from the cavity center and, hence, it matches the undulator center. This can be seen in Fig. 2A where the diameter of the Gaussian mode (given by $3.5\sigma = 7\sigma$, where σ and ω denote one and two standard deviations of the Gaussian, respectively) is plotted as a function of the position within the cavity for various wavelengths. The Rayleigh length of the waist equals 1.0 m corresponding to half the undulator length. The cavity mirror diameter of 50 mm is larger than the mode diameters at the mirror positions for all wavelengths. However, as can be seen in Fig. 2A, the vertical clearance of the undulator vacuum chamber of 13 mm is smaller than the mode diameter at both chamber ends for wavelengths longer than 20 μm . The corresponding cavity losses, plotted in Fig. 2B, increase rapidly with wavelength. Therefore, we expect the cavity losses, rather than the maximum undulator parameter, to be the limiting factor for the maximum wavelength for which lasing can be achieved.



Figure 3: IR cavity mirrors for hole-outcoupling. Gold-plated copper mirrors, with different diameters of the outcoupling hole are mounted on a precision translations stage (design by Bestec GmbH, Berlin). The 50-mm-diameter mirrors have a concave spherical surface of 3.51 m radius of curvature.

The cavity losses plotted in Fig. 2B need to be compared with the single-pass small-signal gain. In Fig. 5 we plot the calculated gain as a function of electron energy and undulator parameter for three different electron bunch lengths of 5, 3, and 1 ps (rms). The gain increases significantly with decreasing bunch length and reaches a maximum of more than 200% for a 1 ps short

bunch in the wavelength range between 7 and 30 μm . For a wavelength as long as 60 μm the calculated gain,

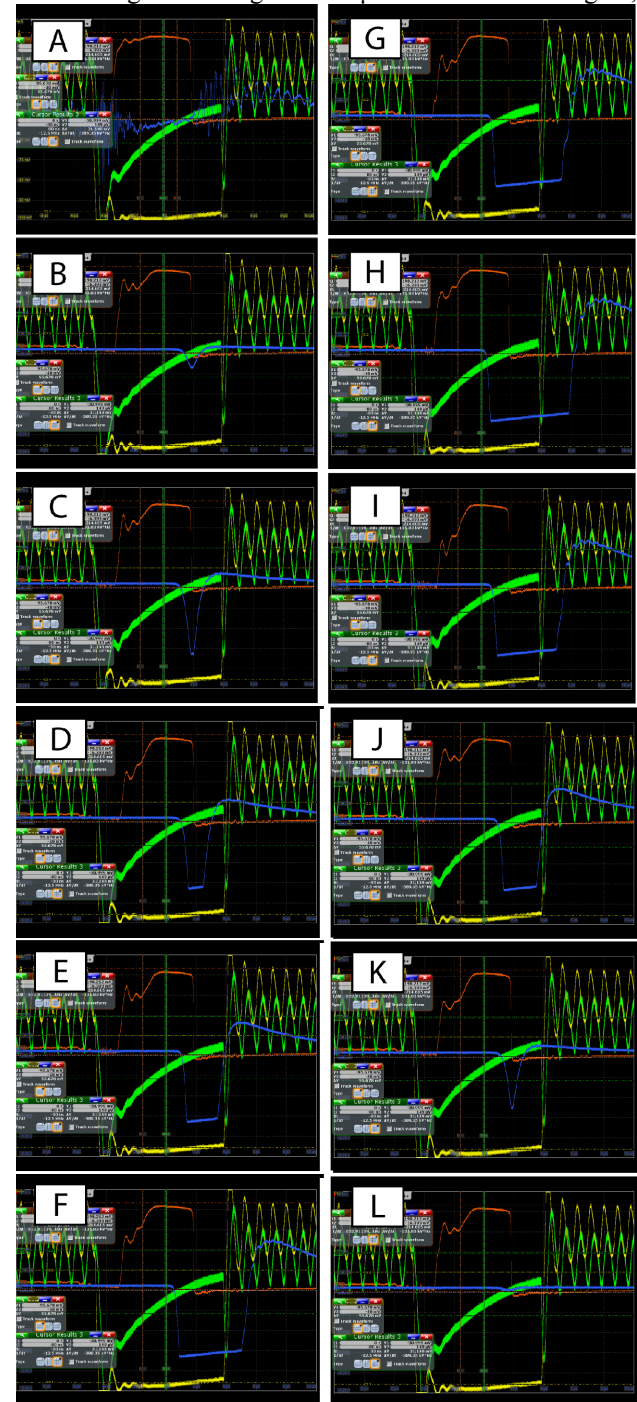


Figure 4: Oscilloscope screenshots from ‘first lasing’. The traces represent the IR detector signal (blue), the electron current (brown), and the phase and amplitude of the RF field in the sub-harmonic buncher cavity (green and yellow, respectively). The abscissa scale spans 20 μs (2 μs per division). The ordinate scale of the blue IR signal is identical from (B) to (L), but zoomed in in (A) to visualize the noise of the IR detector signal in the absence of lasing. Plots (B) to (L) indicate the onset and fading of lasing while the cavity length is increased in steps of 10 μm , hence, in total by 100 μm from (B) to (L).

even for a 3 ps electron bunch, is still more than 75% and, hence, larger than the expected cavity losses. Therefore, we expect a good chance of observing lasing at a maximum wavelength approaching 60 μm .

FIRST LASING RESULTS

To achieve first lasing the undulator was set to a gap of 20 mm corresponding to a peak on-axis magnetic flux-density of 0.46 T and $K_{\text{rms}} = 1.22$ [6]. The electron energy was adjusted to 28 MeV at a current of 200 mA. The latter corresponds to a bunch charge of 200 pC at a repetition

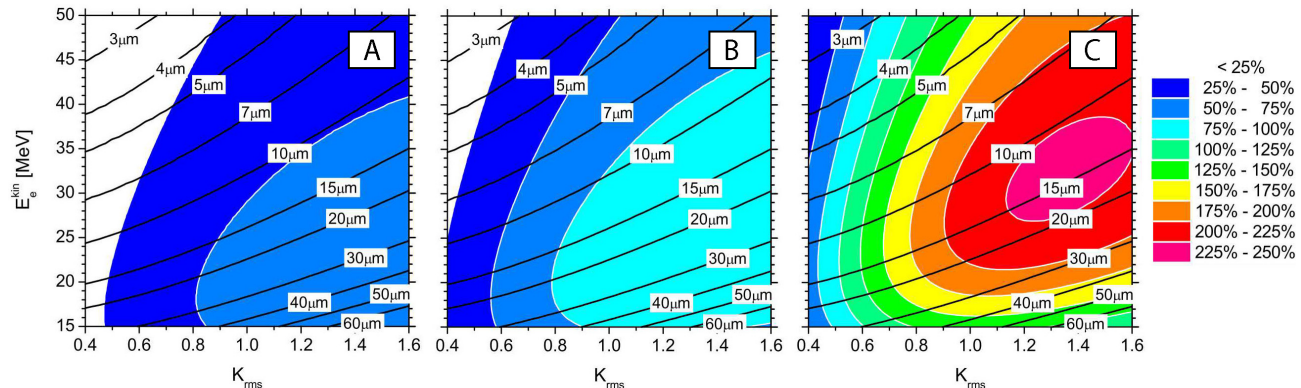


Figure 5: Single-pass small-signal gain calculated for three electron bunch lengths (rms) of (A) 5 ps, (B) 3 ps, and (C) 1 ps. In the calculation a bunch charge of 200 pC, an energy spread of 50 keV, and a normalized transverse emittance of $20 \pi \text{ mm mrad}$ have been assumed.

rate of 1 GHz. As can be seen in Fig. 5, at these conditions we expect lasing at 16 μm with a comparatively high gain even for relatively long electron bunches. The electron beam was aligned to the cavity axis by monitoring the electrons with 4 Beryllium OTR view screens that can be moved into the electron beam path within the undulator vacuum chamber.

To detect the IR radiation, a liquid-nitrogen cooled MCT (HgCdTe) detector was placed about 80 cm downstream from the outcoupling mirror outside the vacuum container. A diamond window mounted under Brewster angle is used to separate the ultra-high vacuum of the cavity chamber from atmosphere, allowing for broadband IR transmission. An outcoupling mirror with a 1.5 mm diameter hole was chosen. The pitch and yaw angles of both cavity mirrors were aligned with a precision of about 0.1 mrad using a HeNe laser.

Fig. 4 shows a series of oscilloscope screenshots for various cavity lengths. In Fig. 4A the cavity length is greatly detuned and the IR signal (blue) just displays noise. From the electron current signal (brown) the macro-bunch length is determined to be about 5.5 μs . The plots B to L were measured by changing the cavity length in steps of 10 μm . The IR signal first rises (B to D) until the MCT detector reaches saturation (D). Further changing the cavity length leads to a broadening of the saturated pulse (D - H) until its width reaches a maximum (H). Subsequently, the pulse gets narrower again (H - J) and, eventually, the signal fades out again (J - L). The total

cavity length change over which lasing is observed (B - L) amounts to 100 μm .

When the IR detector saturates, the end of the pulse appears up to 4 μs after the end of the electron macro-bunch. We attribute this to an artefact of the MCT detector, which needs a longer time to recover, the more the input signal exceeds the saturation threshold. However, the early slope of the saturated IR signal shifts to earlier times (B - H) by almost 1 μs . We interpret this shift as evidence for increasing (B - H) and decreasing (H - L) FEL gain.

SUMMARY AND OUTLOOK

A new mid-infrared FEL has been commissioned at the Fritz-Haber-Institut in Berlin. It will be used for spectroscopic investigations of molecules, clusters, nanoparticles and surfaces. The oscillator FEL is operated with 15 – 50 MeV electrons from a normal-conducting S-band linac equipped with a gridded thermionic gun and a chicane for controlled bunch compression. Calculations of the FEL gain and IR-cavity losses predict that lasing will be possible in the wavelength range from less than 4 to more than 50 μm . First lasing was observed at a wavelength of 16 μm with an electron energy of 28 MeV. At these conditions, lasing was observed over a cavity length scan range of 100 μm . In addition, a second FEL branch covering the FIR/THz regime from 40 to 500 μm has been designed, allowing for a future system upgrade.

REFERENCES

- [1] <http://fel.fhi-berlin.mpg.de/>
- [2] H. Bluem et al., MOPA09, Proc. FEL 2010. <http://accelconf.web.cern.ch/AccelConf/FEL2010/>
- [3] W. Schöllkopf et al., TUPB30, Proc. FEL 2011. <http://accelconf.web.cern.ch/AccelConf/FEL2011/>
- [4] A.M.M. Todd et al., THP043, Proc. PAC 2011. <http://accelconf.web.cern.ch/AccelConf/PAC2011/>
- [5] H. Bluem et al., WEOC04, these proceedings. <http://accelconf.web.cern.ch/AccelConf/FEL2012/>
- [6] S.C. Gottschalk et al., THPD13, these proceedings. <http://accelconf.web.cern.ch/AccelConf/FEL2012>